Suppression of Void Nucleation by Injected Interstitials During Heavy Ion Bombardment

D.L. Plumton and W.G. Wolfer

August 1984

UWFDM-588

J. Nucl. Mat. 120, 245-253 (1984).

FUSION TECHNOLOGY INSTITUTE

UNIVERSITY OF WISCONSIN

MADISON WISCONSIN

Suppression of Void Nucleation by Injected Interstitials During Heavy Ion Bombardment

D.L. Plumton and W.G. Wolfer

Fusion Technology Institute
University of Wisconsin
1500 Engineering Drive
Madison, WI 53706

http://fti.neep.wisc.edu

August 1984

UWFDM-588

J. Nucl. Mat. 120, 245-253 (1984).

SUPPRESSION OF VOID NUCLEATION BY INJECTED INTERSTITIALS DURING HEAVY ION BOMBARDMENT

D.L. Plumton

W.G. Wolfer

Fusion Engineering Program
Nuclear Engineering Department
University of Wisconsin-Madison
Madison, Wisconsin 53706

August 1984

UWFDM-588

1. Introduction

Ion bombardment has been in use for over a decade now as a tool to study radiation damage and void swelling in metals. As an irradiation technique, it has the advantage of obtaining data on void swelling with considerable savings in time and money compared to neutron irradiation experiments. However, the nonuniform damage distribution has been considered a disadvantage. The development of the cross section procedure [1,2] for the post-irradiation examination has turned this disadvantage into a considerable asset of the technique; it is now possible to obtain void swelling data for different displacement rates from one sample. This increase in experimental sophistication has also enabled researchers to examine more closely the variation of void formation and growth as a function of the ion range.

The comparison of ion bombardment results with those obtained from neutron irradiations has revealed significant differences which cannot easily be explained based only on different displacement rates and different temperatures. First, swelling as a result of ion bombardment is often found to saturate at levels ranging from a few percent to several tens of a percent; in contrast, no saturation is found for comparable neutron irradiations. Second, the steady state swelling rate per dpa appears to be significantly lower than the one for neutron irradiated materials. Furthermore, this rate seems to depend on the depth [3]. There are additional differences, e.g. a denuded zone near the front surface, and the presence of an inevitable compressive stress in the bombarded layer.

Rate theory has been used to demonstrate that an increase in displacement rate leads to a shift of the temperature range over which swelling occurs [4]. However, no difference in the steady state swelling per dpa would be expected.

At low temperatures, where recombination is dominant, the injected interstitials can reduce the void growth rate as shown by Brailsford and Mansur [5]. This reduction is significant only when the bias is small, i.e. when the current of vacancies is almost equal to the current of interstitials into the void. Obviously, this will be the case for voids of the critical size. Therefore, we expect that the injected interstitials will affect void nucleation to a greater extent than void growth.

The effect of injected interstitials on void nucleation depends on the precise distribution of both the displacement damage and the deposited ions. For a large ion range, such as exists in 14 MeV Ni ion bombardment of nickel, the region of mutual overlap of these distribution profiles is relatively small and not very sensitive to the precise determination of these profiles. However, for lower energy bombardment the overlap region becomes an increasing fraction of the total ion range. Consequently, any inaccuracies in the damage and ion deposition profiles for low energy ions, such as 5 MeV Ni on nickel, will likely have a large effect on the accuracy of the nucleation profile. These expectations led to the study reported in the present paper.

The organization of the paper is as follows: we review first in Section 2 the void nucleation theory as originally developed by Katz and Wiedersich [6], Russell [7], and as further refined by Si-Ahmed and Wolfer [8], into which we incorporate the effect of injected interstitials. Numerical results are presented in Section 3 for the void nucleation rate as a function of temperature, displacement rate, rate of injected interstitials, and incident ion energy; both 14 and 5 MeV Ni on nickel are considered. Since the displacement rate and rate of injected interstitials are dependent on the depth, detailed results will be given for the void nucleation as a function of depth.

The results are then discussed and compared with experimental observations in Section 4.

2. Void Nucleation With Injected Interstitials

The steady state void nucleation rate in the presence of supersaturations for both vacancies and interstitials is governed by the quantity

$$\Delta G(x) = -kT \sum_{j=2}^{x} \ln \left[(\alpha(j) + \gamma(j))/\beta(j-1) \right] \tag{1}$$

which represents the nonequilibrium counterpart of the Gibbs free energy for a vacancy cluster containing x vacancies. In contrast to its conventional definition for thermodynamic equilibrium, this energy is determined by the reaction rates $\alpha(j)$, $\beta(j)$, and $\gamma(j)$ for interstitial absorption, vacancy absorption, and vacancy re-emission, respectively, at a cluster containing j vacancies. These reaction rates depend in turn on the average point defect concentration as given by

$$\alpha(x) = 4\pi r(x)\, Z_i^o(x)\, D_i C_i \tag{2}$$

$$\beta(x) = 4\pi r(x)\, Z_v^o(x)\, D_v C_v \tag{3}$$

$$\gamma(x) = 4\pi r(x)\, Z_v^o(x)\, D_v C_v^o(x) \tag{4}$$

where $r(x)$ is the void radius, $Z_i^o(x)$ and $Z_v^o(x)$ are the void bias factors for interstitial and vacancy capture, and D_i and D_v are the diffusion coefficients for interstitial and vacancy migration. If $W(x) = 4\pi r^2(x)\gamma_o$ represents the surface energy of a void, where γ_o is the specific surface energy, and p the

gas pressure inside the void, then

$$C_v^o(x) = C_v^{eq} \frac{Z_v^o(x-1)}{Z_v^o(x)} \frac{r(x-1)}{r(x)} \exp[(W(x) - W(x-1) - p\Omega)/kT] \qquad (5)$$

where Ω is the volume per atom.

The concentration of interstitials and vacancies, C_i and C_v, is given by the solution to the usual rate equations. However, in the present paper the rate of interstitial production, P_i, as a result of both displacement damage and injection, is different from the rate of vacancy production, P_v, so that

$$D_i C_i = D_v \bar{Z}_v F \qquad (6)$$

and

$$D_v C_v = D_v(\bar{Z}_i F + \bar{C}_v) - (P_i - P_v)/\bar{Z}_v S \ . \qquad (7)$$

Here, S is the total sink strength, $\bar{Z}_i$ and $\bar{Z}_v$ are the sink averaged interstitial and vacancy bias factors, and $\bar{C}_v$ is the average vacancy concentration in thermodynamic equilibrium with the sinks. Note that the vacancy concentration (such as $C_v^o(x)$) in local thermodynamic equilibrium with a particular sink type (such as a void of size x) differs both from $\bar{C}_v$ and from C_v^{eq}; the latter is the equilibrium concentration in an ideal crystal.

Equations (6) and (7) contain the quantity

$$F = \frac{S}{2\kappa D_v} \{\sqrt{(1+M)^2 + L} - (1+M)\} \qquad (8)$$

where

$$M = \kappa D_v \bar{C}_v/(\bar{Z}_i S) - \kappa(P_i - P_v)/(\bar{Z}_i \bar{Z}_v S^2) \qquad (9)$$

$$L = 4\kappa P_i/(\bar{Z}_i\bar{Z}_v S^2) \tag{10}$$

and

$$\kappa = 8\pi a_o/D_v \tag{11}$$

with a_o being the lattice parameter.

When the injected interstitials are absent as in neutron or electron irradiations, then $P_i - P_v = 0$, and the above equations reproduce those given earlier [8].

The determination of $\Delta G(x)/kT$ allows the steady state nucleation rate to be computed by the equation

$$I_s = \{\sum_{x=1}^{N-1} \beta^{-1}(x) \exp[-\Delta G(x)/kT]\}^{-1} \tag{12}$$

where N is a cluster size large compared to the critical void size; the latter is defined by the maximum of $\Delta G(x)$.

As shown previously [8], the void nucleation rate is critically dependent upon the void bias factors $Z_i^o(x)$ and $Z_v^o(x)$ which are given by

$$Z^o(x) = Z^b(x)/[1 + \frac{h}{r + h}\,(e^{\Delta u^*/kT} - 1)]\ . \tag{13}$$

This equation is an entirely adequate approximation to the more elaborate formulae given earlier [8,9]. Here, h(x) is the effective thickness of the segregation region around a void of radius r(x), $Z^b(x)$ is the bias factor of a bare void [9] and

$$\Delta u^* \cong \frac{2(1 + \nu)\mu\Omega}{(1 - 2\nu)}\left[\frac{1}{9}\left(\frac{v}{\Omega}\right)^2 \frac{\Delta\mu}{\mu} + \left(\frac{v}{\Omega}\right)\frac{\Delta a_o}{a_o}\right] - \frac{(1 + \nu)\Omega}{3(1 - \nu)}\left(\frac{2\gamma_o}{r} - p\right)\left(\frac{v}{\Omega}\right)\frac{\Delta\mu}{\mu} \tag{14}$$

is the effective barrier energy of the segregation region. Here, ν is the Poisson's ratio, μ the shear modulus of the matrix, and v is the relaxation volume of the point defect. In the segregation region, the shear modulus differs by $\Delta\mu$, and the lattice parameter by Δa_o from the corresponding average values in the matrix.

3. Results

The effect of injected interstitials on void nucleation will be expressed in terms of the parameter ε_i which is equal to the ratio of the injected interstitials to the interstitials produced by displacements. The total interstitial production rate is then given by

$$P_i = P_v(1 + \varepsilon_i) \tag{15}$$

where P_v is equal to the displacement rate times the survival fraction, n, for in-cascade recombination.

The physical parameters listed in Table I, used for the numerical evaluation of the void nucleation rate, represent appropriate values for nickel and austenitic stainless steels. The self-atom diffusivity must be internally consistent so that a change in the vacancy migration energy affects not only the exponential but also the pre-exponential. The formalism used is that developed by Seeger and Mehrer [10] where the pre-exponential, D_{vo}, is treated as a function of the vacancy migration energy.

The parameters for the void segregation shell were chosen so that the void nucleation rate in the absence of injected interstitials, at T = 525°C and for a dose rate of 10^{-3} dpa/s, was equal to about 10^{14} voids/cm^3-s, a

TABLE I. Materials Parameters

Parameter	Value	Dimension
Lattice parameter, a_o	0.352	nm
Surface energy, γ_o	1.0	J/m^2
Shear modulus, μ	10^5	MPa
Poisson's ratio, ν	0.3	---
Vacancy formation energy, E_v^f	1.8	eV
Vacancy migration energy, E_v^m	1.1	eV
Pre-exponential factor, $D_{vo} = a_o \sqrt{E_v^m/M}$	1.29×10^{-6}	m^2/s
Mass of nickel, M	58.7	amu
Vacancy migration entropy[a], S_v^m	1.0 k	---
Vacancy formation entropy[a], S_v^f	1.5 k	---
Interstitial relaxation volume[b], v_I	1.4 Ω	---
Vacancy relaxation volume[b], v_v	-0.2 Ω	---
Interstitial polarizability, α_I^G	150	eV
Vacancy polarizability, α_V^G	15	eV
Modulus variation, $\Delta\mu/\mu$	5×10^{-4}	---
Lattice parameter variation, $\Delta a_o/a_o$	5×10^{-4}	---
Cascade survival fraction, η	0.25	---
Sink strength, S	10^{14}	m^{-2}
Bias factor ratio, $\bar{Z}_I/\bar{Z}_V$	1.2	---
Thickness of segregation shell, h/r	0.1	---

[a]In units of the Boltzmann constant k.

[b]In units of the atomic volume $\Omega = a_o^3/4$.

value comparable to the observed one in the nickel ion-bombardment experiments on nickel [3].

The effect of various amounts of injected interstitials, in the range ε_i = 0 to 10^{-3}, gives the void nucleation rates shown in Figs. 1, 2 and 3 as a function of temperature. It is clearly seen that when the injected interstitials exceed 0.01% of those produced by displacements, void nucleation is severely suppressed at low temperatures. In fact, there exists a temperature threshold below which void nucleation does not occur at all. This threshold depends on the injected interstitial fraction ε_i, the dose rate (Figs. 1 and 2), the vacancy migration energy (Figs. 1 and 3), and to a lesser extent on the sink strength. The results of Figs. 1-3 indicate that the most severe suppression of void nucleation is expected in regions of maximum damage production where most of the injected interstitials come to rest. If the dose rate is increased from 10^{-3} to 10^{-2} dpa/s, Figs. 1 and 2, the threshold temperature and void nucleation peak shift towards higher temperature and the suppression of void nucleation by the excess interstitials increases. If the vacancy migration energy is assumed to be 1.4 eV (and if the vacancy formation energy is reduced so as to keep the activation energy for self-diffusion constant at 2.9 eV) the results shown in Fig. 3 are obtained. It is seen that the void nucleation rates are reduced compared to the results shown in Fig. 1, while the threshold temperatures are increased. An increase in the vacancy migration energy or in the displacement rate simply shifts the curves to higher temperatures and lower nucleation rates.

Due to the strong dependence on displacement rate, the suppression of void nucleation needs to be evaluated for the particular ion-bombardment of interest and as a function of depth. The cases examined here are 14 MeV and 5

MeV Ni-ion bombardment of nickel. Displacement rates and the fraction ε_i of injected interstitials were computed with the BRICE code [11] for both the 14 MeV and 5 MeV case while the HERAD code [12] was used for just the 5 MeV case. The 14 MeV results will be examined first and then the 5 MeV results.

Figure 4 illustrates the displacement rate and excess interstitial fraction as a function of depth obtained from the BRICE code results for the 14 MeV case. Only the depth region around the end of the range is shown in this and the following figures as this is the region of interest for the present investigation. Using the displacement rates of Fig. 4, the void nucleation rates shown in Fig. 5 are obtained where dashed lines are nucleation rates without the inclusion of the injected interstitials. As a function of depth, the void nucleation rates without injected interstitials follow the profile of the displacement rate. However, since a variation in the displacement rate with depth is equivalent to a "temperature shift", the void nucleation rates for the lower temperatures do not decrease as drastically on either side of the peak damage region as one would expect.

If the injected interstitials are now included in the void nucleation calculations, the solid lines shown in Fig. 5 are obtained. At the temperatures of 300 and even 400°C a depression of the void nucleation becomes noticeable where the fraction ε_i of injected interstitials is greatest. Since void nucleation is sensitive to the sink strength, cascade survival fraction, vacancy migration energy, etc., the depression should also be strongly dependent on these parameters. Accordingly, several parametric studies were done.

For example, recent measurements of the vacancy formation energy by the positron annihilation technique have yielded a value of 1.8 ± 0.1 eV [13], which is significantly larger than the previously established value. Since

the value of self-diffusion energy remains unaltered it implies a vacancy migration energy for nickel of 1.1 ± 0.1 eV. This value then agrees closely with the recently measured value of 1.04 ± 0.04 eV for the Stage III activation energy [14]. Suppose now that the vacancy migration energy is 1.2 eV, which shifts E_v^f to 1.7 eV, instead of the 1.1 eV used for the results in Fig. 5. As Fig. 6 shows, the suppression of void nucleation becomes more pronounced. Furthermore, if we reduce the sink strength from 10^{14} m^{-2} to 5 x 10^{13} m^{-2}, the gap in void nucleation increases even further as shown in Fig. 7.

The calculations for 5 MeV Ni ion bombardment of nickel were carried out using the results of both the BRICE [11] and the HERAD [12] code. It is assumed in the BRICE code that the ion deposition profile is Gaussian. While this is probably a reasonable assumption for high energies, it is expected to be less reliable at lower ion energies. The HERAD code solves the ion transport problem without resorting to any compromising assumptions by the implementation of a Monte Carlo simulation. With a sufficiently large number of case histories, accurate damage and ion deposition profiles can be obtained.

The displacement damage profiles, for 5 MeV Ni on nickel, calculated with the BRICE and HERAD codes are illustrated in Figs. 8 and 9, respectively, where the minimum displacement energy is taken as 40 eV. The damage peak for the BRICE case is at ~ 0.85 μ while for the HERAD case the peak is at ~ 1.05 μ. This shift of the HERAD peak, relative to the BRICE peak, towards the end of range is reflected in the ion deposition profiles. The BRICE peak deposition is at ~ 1 μ while the HERAD peak deposition is at ~ 1.2 μ.

The displacement rate and the excess interstitial fraction for 5 MeV Ni ions are plotted as a function of depth for both codes in Fig. 10. The excess

interstitial fraction in both 5 MeV cases rises to about three times the magnitude of that in the 14 MeV case. Therefore the excess interstitials should be more important for 5 MeV irradiations than the 14 MeV irradiations.

The depth and temperature dependence of the void nucleation rates for 5 MeV Ni on nickel is shown in Fig. 11 for the BRICE code, and in Fig. 12 for the HERAD code. The dashed lines in both figures again represent void nucleation rates with injected interstitials neglected. The suppression of void nucleation is seen to be very significant except for the high temperature, 600°C, cases. Some discrepancies in the void suppression between the BRICE and HERAD code are observed. The damage and ion deposition profiles from both codes result in a similar suppression at their respective damage peaks. However, the suppression predicted in the near surface region at low temperatures is significantly larger using HERAD data as compared to the BRICE data.

The shift in the void nucleation peak due to excess interstitial suppression can be larger for the HERAD code than for the BRICE code depending on the temperature. The BRICE code results give a peak nucleation shift of ~ 0.4 μ at 300°C (0.9 μ to 0.5 μ) while at 500°C the shift is ~ 0.3 μ (0.9 μ to 0.6 μ). The HERAD code results give a peak nucleation shift of ~ 1 μ at 300°C (1.1 μ to 0.1 μ) while at 500°C the shift is ~ 0.3 μ (1.1 μ to 0.8 μ).

4. Discussion

The suppression of void nucleation by the injected interstitials is most effective when their number becomes a significant fraction of the number of interstitials which have escaped recombination both in the cascade and in the bulk. Accordingly, the suppression is found where the ions are deposited and where recombination is the predominant fate of point defects. These conditions are identical to those valid for void growth suppression [4]. The

difference lies merely in the magnitude of the suppression; it is much more dramatic for void nucleation than for void growth.

If void swelling after ion bombardment is measured either from step heights or by microscopic examinations in the peak damage region the effect of the injected interstitials is present. The swelling-temperature relationship obtained by these two techniques exhibits a sharply peaked behavior with a precipitous decline in swelling towards lower temperatures around 400°C to 500°C, depending on the displacement rate [15]. Our present results suggest that the suppression of swelling for these lower temperatures is due, in part, to the effect of injected interstitials on void nucleation.

The existence of a void free gap in the depth distribution has been discovered experimentally by Whitley [3]. Figure 13 shows the depth distribution of the void density in nickel irradiated with 14 MeV Cu ions at a temperature of 400°C, where it was found that voids nucleate in two separate bands, one found in front and one behind the peak damage region. Although a large fraction of the self-ions come to rest behind the peak damage region, void nucleation is still possible in spite of the high concentration of excess interstitials because the displacement rate is low. The low displacement rate gives a low supersaturation so that point defect loss occurs mainly at sinks and recombination is insignificant as a loss mechanism; therefore the injected interstitials have little effect on void nucleation.

While the present theoretical predictions on the depth distribution of void nucleation for 14 MeV Ni on nickel agree in principle with this observation of a void free gap, there are quantitative differences. First, the extent of the observed gap is larger than the predicted ones. Second, the deepest void region in this experiment is in fact beyond the end of range as

computed with the BRICE code. Apart from the latter discrepancy, a direct quantitative comparison between the above experimental observation and the theoretical results cannot strictly be made for the following reasons.

The observed void distribution reflects both the processes of nucleation and growth to a visible size. In contrast, the computed nucleation rates must be interpreted in terms of a depth distribution for voids larger than the critical size, regardless of how small. The critical size is generally below the limit of visibility for transmission electron microscopy. Another difference arises from our assumption of a spatially uniform sink strength. Even though this is justified with regard to the initial distribution of grown-in dislocations, irradiation quickly produces a spatially nonuniform distribution of dislocation loops prior to void nucleation. Consequently, the void nucleation calculations should be carried out with this nonuniform distribution of the total dislocation density as obtained at low doses. Unfortunately, this information is not presently available. Finally, diffusional spreading of vacancies and interstitials is not accounted for in the present calculations. Recent work by Farrell et al. [16] has shown that void formation and growth is observed at depths significantly larger than the computed displacement damage profile, and that this extension of the swelling range is in good agreement with calculations by Mansur and Yoo [17] on diffusional spreading.

For 5 MeV Ni on nickel the void nucleation differences, obtained between the BRICE code and the HERAD code, occurs because of the difference in the shape of the displacement rate and ion deposition profiles. The BRICE code gives a Gaussian shape while the HERAD code gives a non-Gaussian shape exhibiting a more pronounced tail towards the surface. Because of the more detailed physical modeling of the collision process in HERAD and the absence

of any compromising assumptions regarding the solution of the transport equation, the results of the HERAD code are expected to be more reliable.

The larger suppression of void nucleation at (or near) the peak damage region in the BRICE case occurs because the ion-deposition profile does not exhibit straggling as in the HERAD case. On the other hand, the larger shift in the nucleation peak in the HERAD case is a result of more straggling towards the surface as compared to the BRICE case. The long tail towards the surface gives a low excess interstitial fraction which is only significant at low temperatures when recombination dominates the point defect loss.

Regardless of which code is used, the effects of injected interstitials at this medium energy, 5 MeV, are more pronounced than in the 14 MeV results because the excess interstitials cover a larger fraction of the total range. When a more accurate displacement damage code such as HERAD is used the effect of injected interstitials is larger in the low temperature range than might be expected strictly from analysis with the BRICE code.

Garner has recently shown that injected interstitials have a pronounced effect on self-ion-induced swelling, leading both to an extension of the transient regime of swelling and to a suppression of the steady state swelling rate [18]. He also demonstrated that the strongly peaked swelling distributions characteristic of ion irradiations were not typical of neutron irradiations and attributed the divergence to the injected interstitial. He noted, however, that within the confines of available theory, the injected interstitials were insufficient to affect the steady state swelling rate.

A reduction in the magnitude of the vacancy migration energy from 1.4 to 1.1 eV strongly reduces the predicted influence of injected interstitials on the swelling rate [17], and we have shown that it also decreases the suppres-

sion of void nucleation by injected interstitials. Therefore, the work presented in this paper provides a qualitative explanation for the observed difference in the low temperature dependence of neutron and ion-induced swelling. The possible suppression of the steady-state swelling rate in ion-bombardment at higher temperatures [19] can, however, not be explained by the present theoretical results or by the injected interstitial effect on void growth as predicted by Brailsford and Mansur [5].

Acknowledgments

We thank Dr. H. Attaya for providing us with the HERAD displacement calculations and for discussions on differences between his and the BRICE code. This work was supported by the U.S. Department of Energy under contracts DE-AC02-82ER52082 and DE-AC02-78ET52019 with the University of Wisconsin.

References

[1] R. A. Spurling, C. Rhodes, J. Nucl. Mat. 44 (1972) 341.

[2] J. B. Whitley, G. L. Kulcinski, P. Wilkes, and H. V. Smith, Jr., J. Nucl. Mat. 7 (1979) 159.

[3] J. B. Whitley, Ph.D. Thesis, University of Wisconsin, 1978.

[4] A. D. Brailsford, R. Bullough, J. Nucl. Mat. 44 (1972) 121.

[5] A. D. Brailsford, L. K. Mansur, J. Nucl. Mat. 71 (1977) 110.

[6] J. L. Katz, H. Wiedersich, J. Chem. Phys. 55 (1971) 1414.

[7] K. C. Russell, Acta Met. 19 (1971) 753.

[8] A. Si-Ahmed and W. G. Wolfer, ASTM STP 783 (1982) 1008.

[9] W. G. Wolfer and L. K. Mansur, J. Nucl. Mat. 91 (1980) 265.

[10] A. Seeger and H. Mehrer, Vacancies and Interstitials in Metals, ed. by A. Seeger, D. Schumacher, W. Schilling and J. Diehl, North-Holland, Amsterdam, 1970, p. 1.

[11] D. K. Brice, Report SAND 7500622, Sandia National Laboratories, July 1977.

[12] H.M. Attaya, Ph.D. Thesis, University of Wisconsin, 1981.

[13] L. C. Smedskjaer, M. J. Fluss, D. G. Legnini, M. K. Chason, and R. W. Siegel, J. Phys. F: Metal Phys. 11 (1981) 2227.

[14] S. K. Khana and K. Sonnenberg, Rad. Effects 59 (1981) 91.

[15] W. G. Johnston, J. H. Rosolowski, A. M. Turkalo, and T. Lauritzen, J. Nucl. Mat. 47 (1973) 155.

[16] K. Farrell, N.H. Packan, and J.T. Houston, Rad. Effects 62 (1982) 39.

[17] L.K. Mansur and M.H. Yoo, J. Nucl. Mat. 85 and 86 (1979) 523.

[18] F.A. Garner, "Impact of the Injected Interstitial on the Correlation of Charged Particle and Neutron-Induced Radiation Damage," Proceedings of AIME Symposium on Radiation Damage Analysis for Fusion Reactors, October 24-28, 1982, St. Louis, MO (to be published in J. Nucl. Mat.); also in DAFS quarterly report (DOE/ER-0046/11).

[19] E.H. Lee, L.K. Mansur, and M.H. Yoo, J. Nucl. Mat. 85 and 86 (1979) 577.

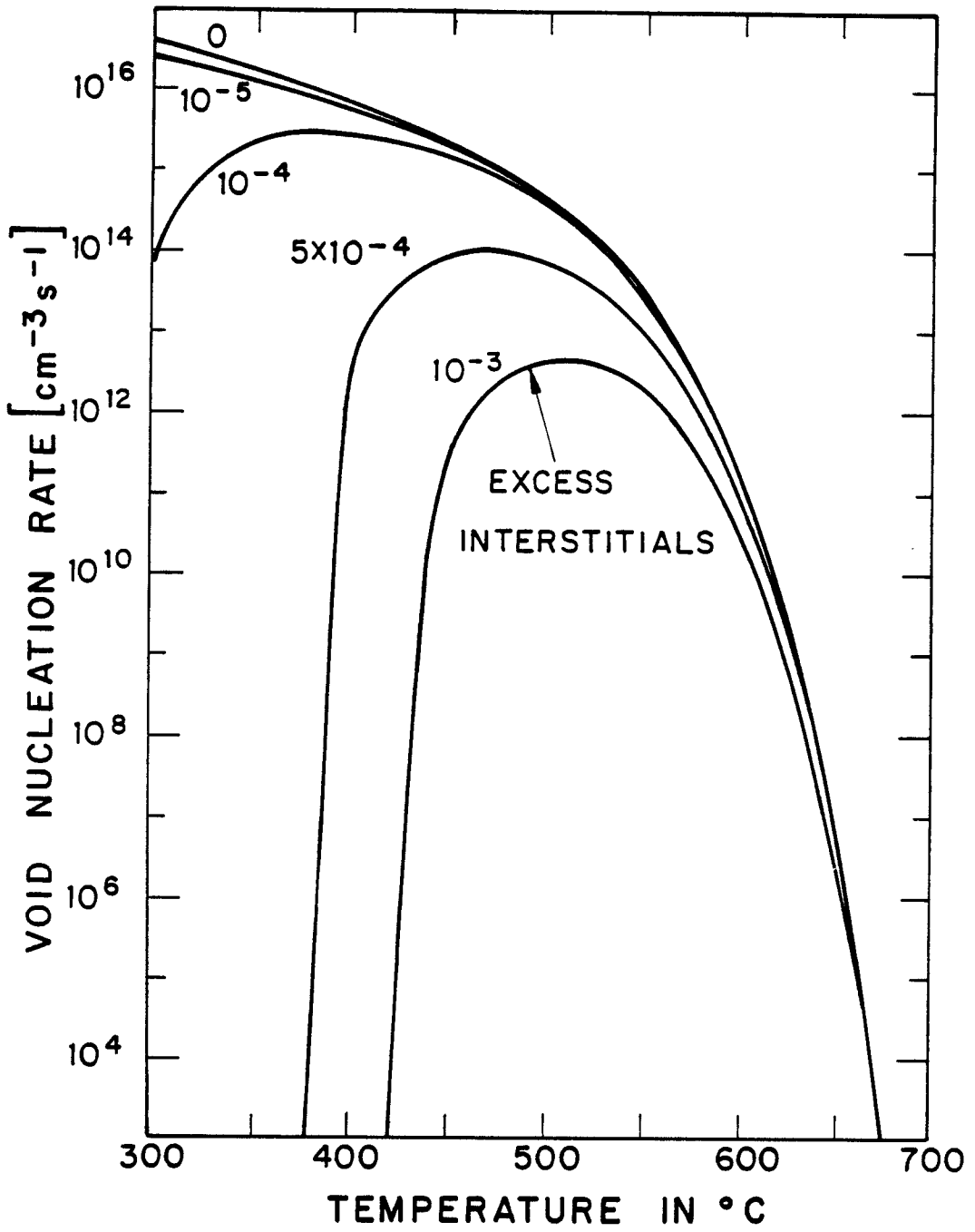

Fig. 1. Void nucleation rate for a displacement rate of 10^{-3} dpa/s; vacancy migration energy of 1.2 eV; sink strength of 5 x 10^{13} m^{-2}.

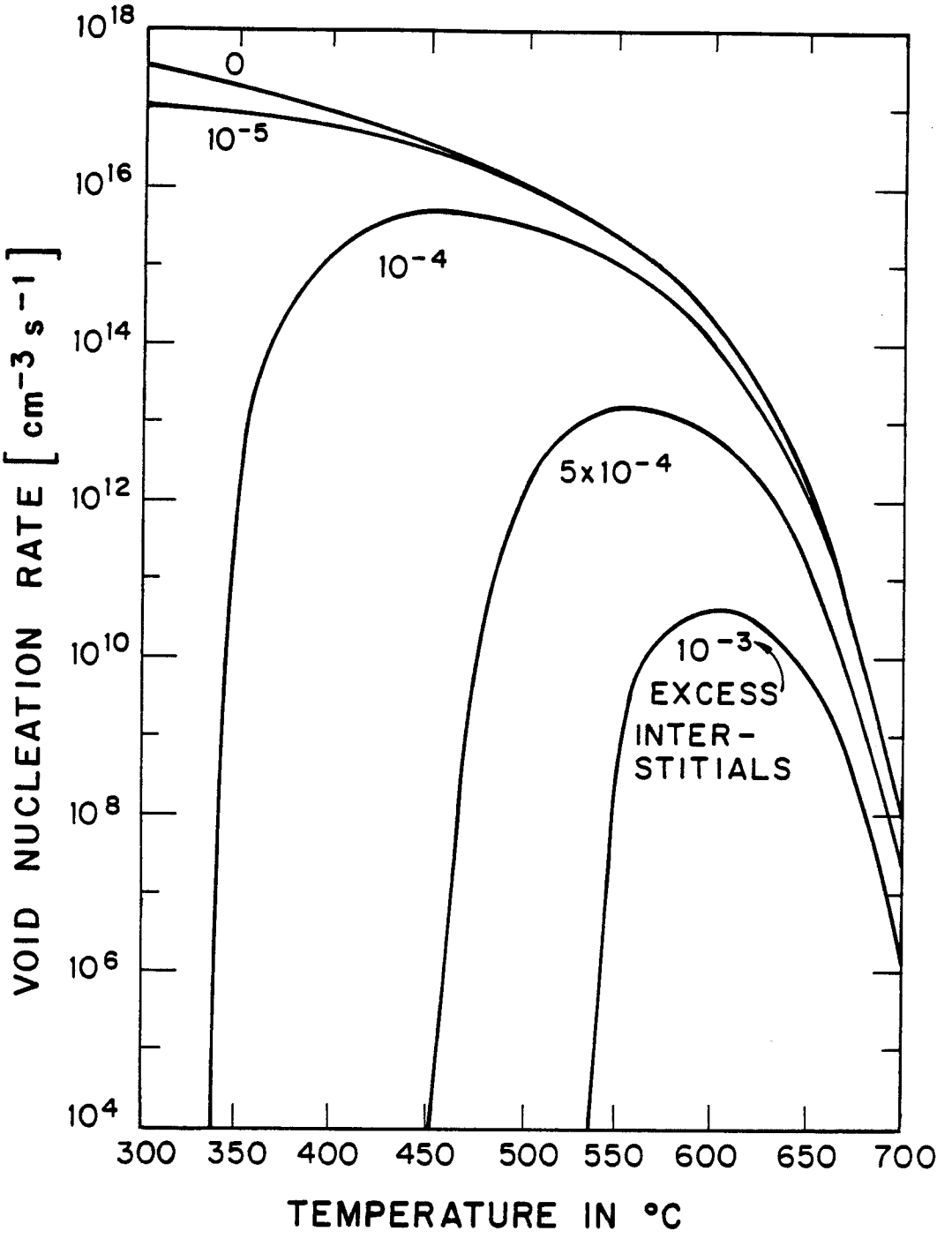

Fig. 2. Void nucleation rate for a displacement rate of 10^{-2} dpa/s; all other materials parameters as in Fig. 1.

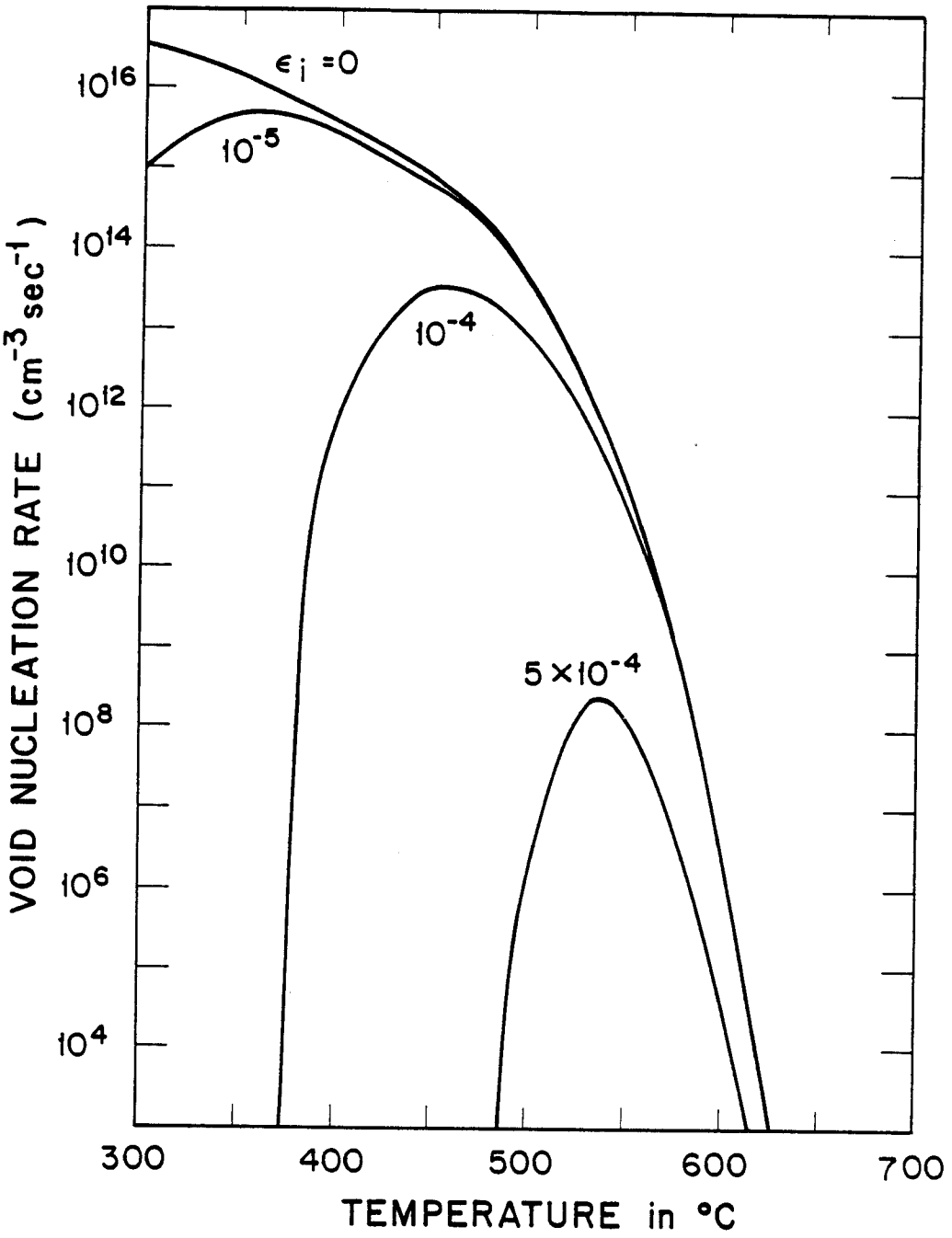

Fig. 3. Void nucleation rate for a displacement rate of 10^{-3} dpa/s; vacancy migration energy of 1.4 eV; sink strength of 5×10^{13} cm^{-2}.

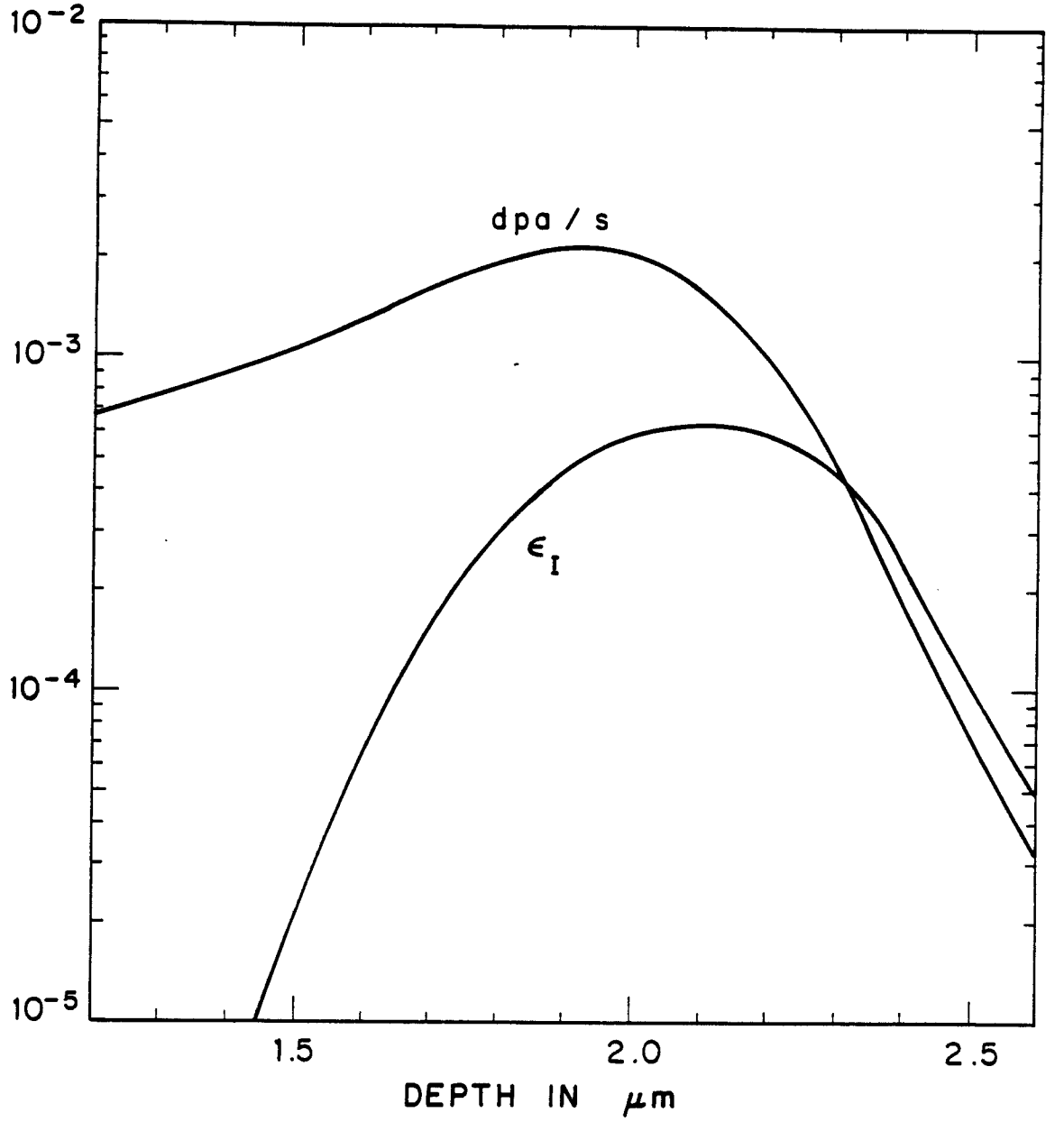

Fig. 4. Depth distribution of the displacement rate and injected interstitial fraction for 14 MeV Ni-ions on Ni according to the BRICE code.

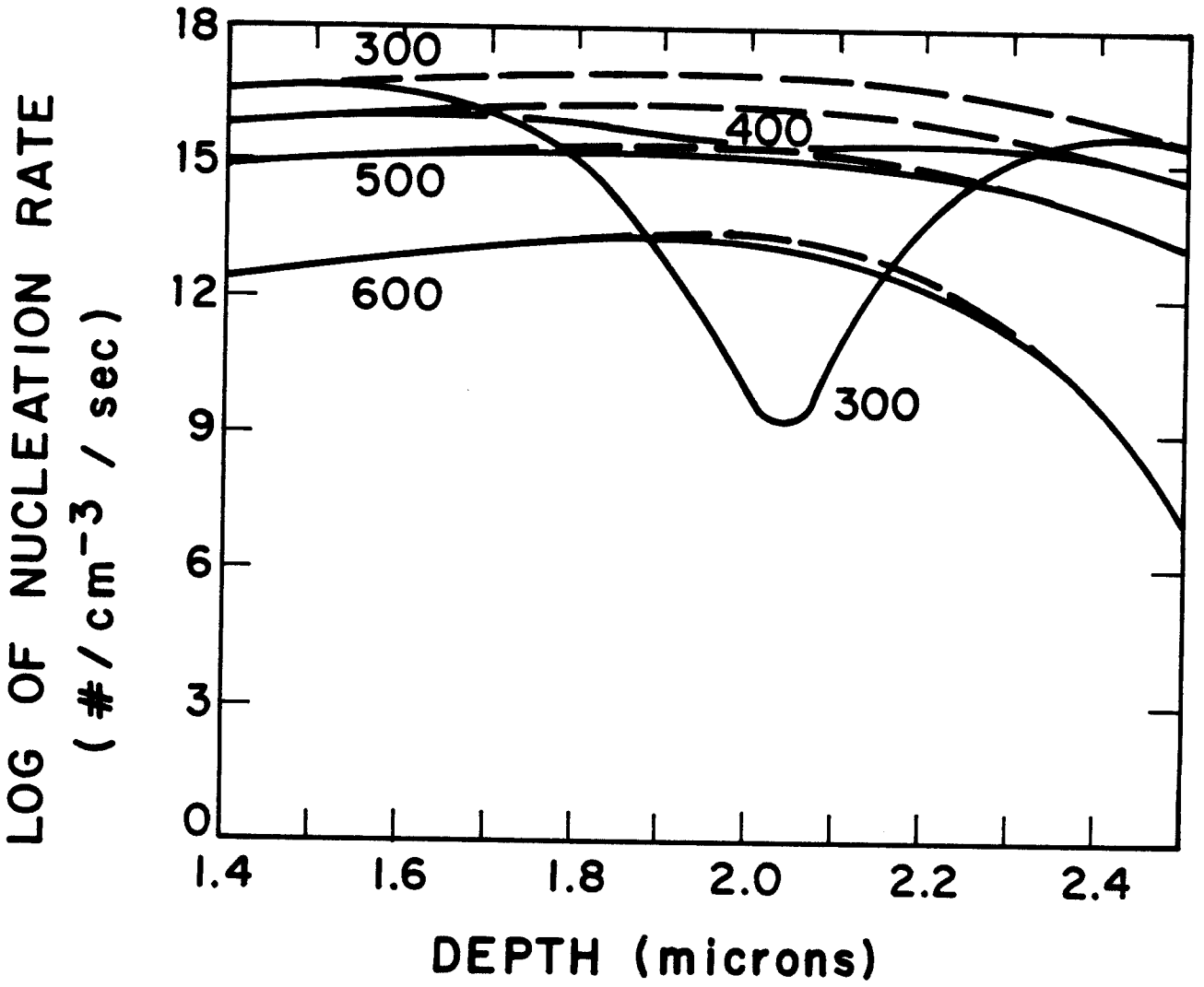

Fig. 5. Void nucleation rate with and without injected interstitials vs. depth; for 14 MeV Ni-ions; sink strength of 10^{14} m^{-2}; vacancy migration energy of 1.1 eV.

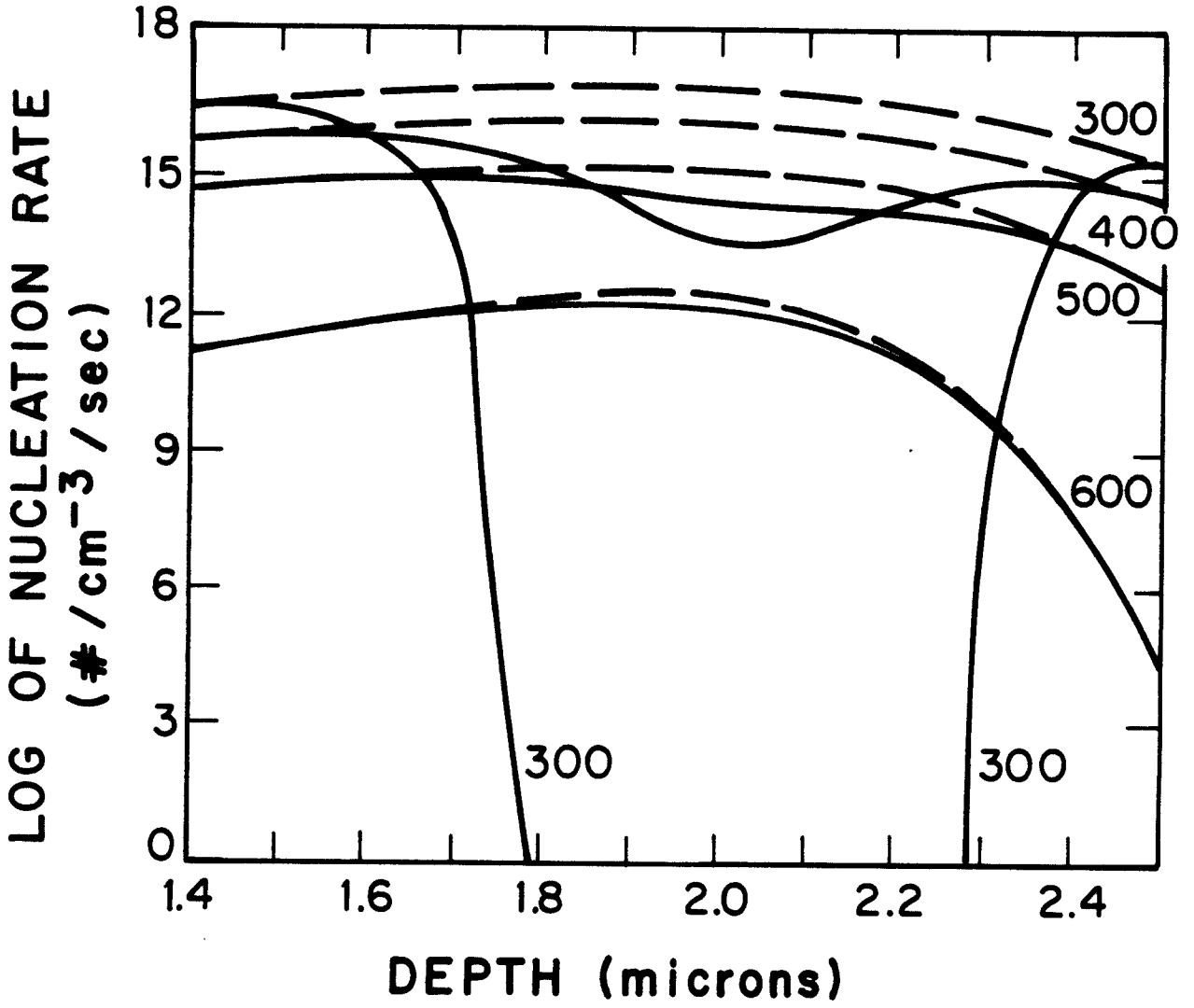

Fig. 6. Void nucleation rate vs. depth; vacancy migration energy of 1.2 eV; all other parameters as in Fig. 5.

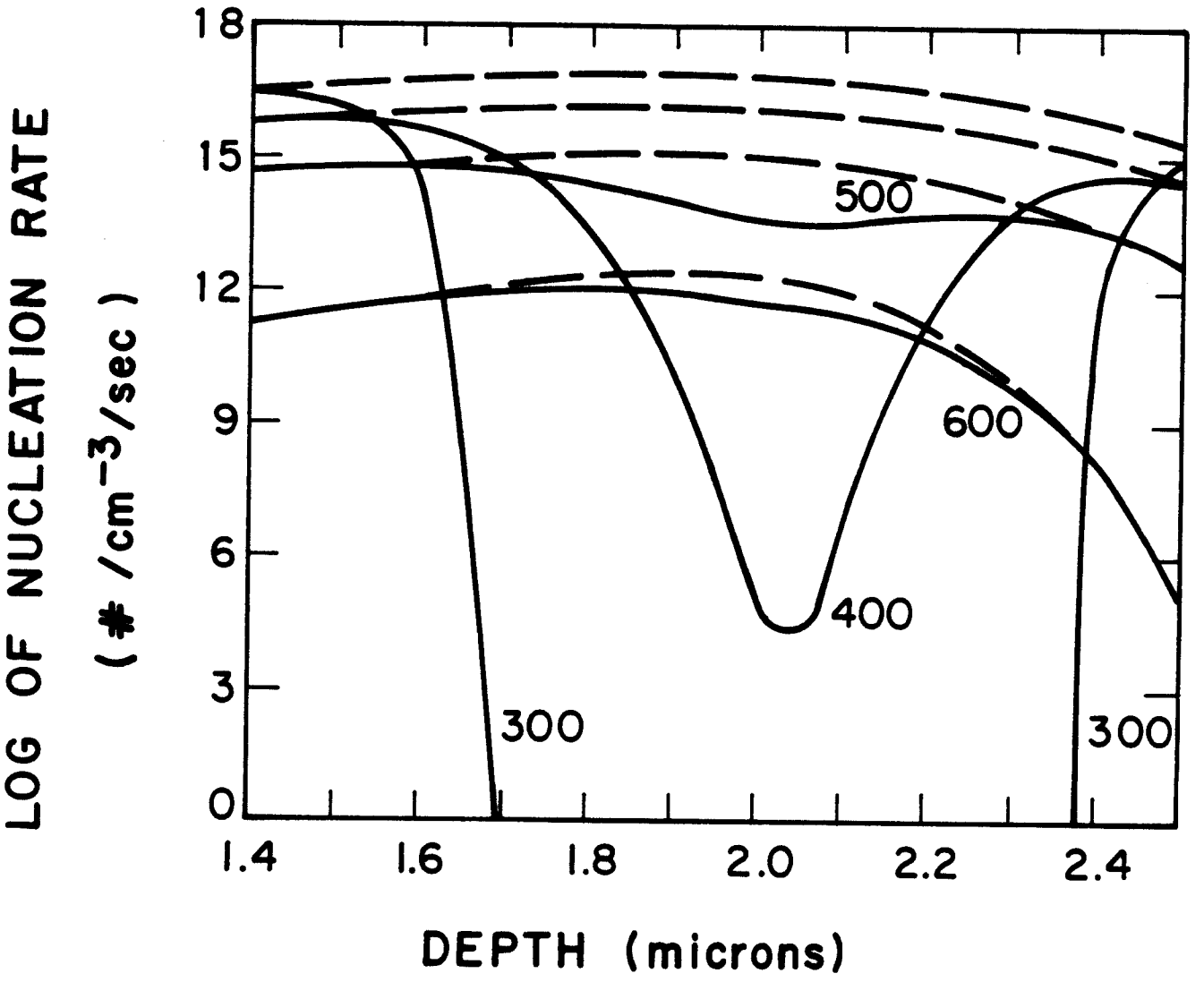

Fig. 7. Void nucleation rate vs. depth; vacancy migration energy of 1.2 eV; sink strength of 5×10^{13} m^{-2}.

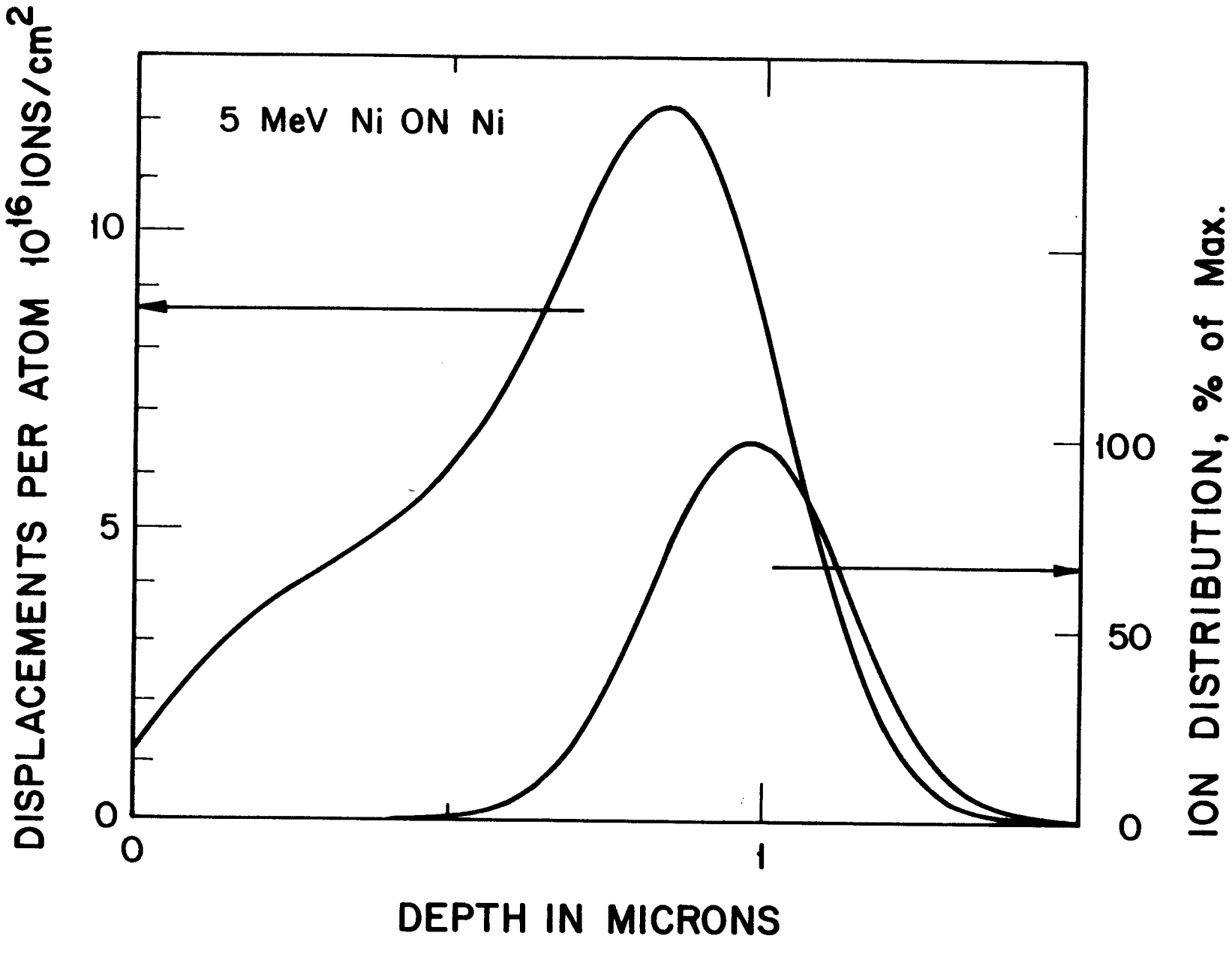

Fig. 8. Displacement damage and ion deposition distribution for 5 MeV Ni on Ni using the BRICE code [11].

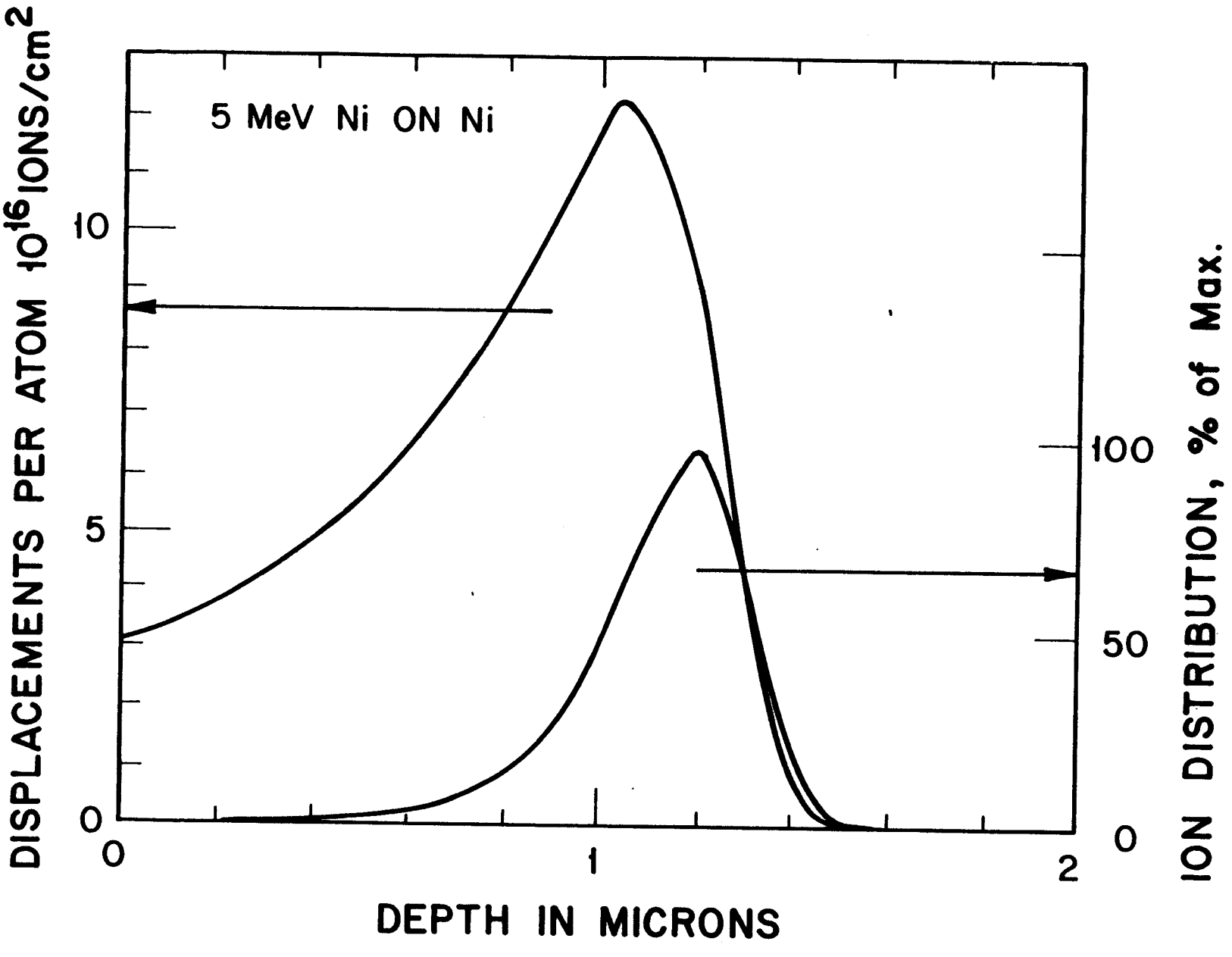

Fig. 9. Displacement damage and ion deposition distribution for 5 MeV Ni on Ni using the HERAD code [12].

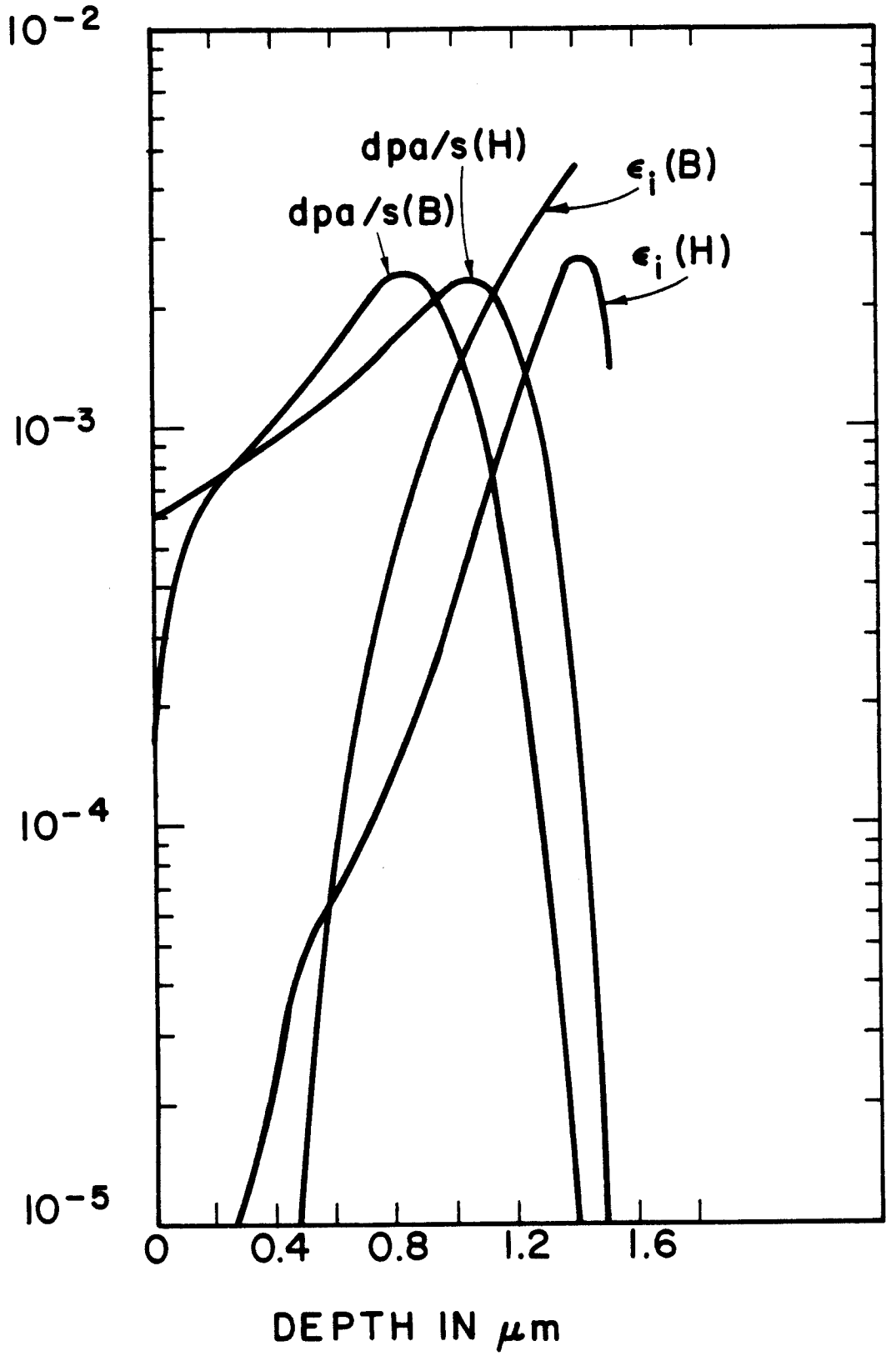

Fig. 10. Comparison of the 5 MeV Ni on nickel displacement rates and excess interstitial fraction, ϵ_i, between the BRICE (B) code and the HERAD (H) code.

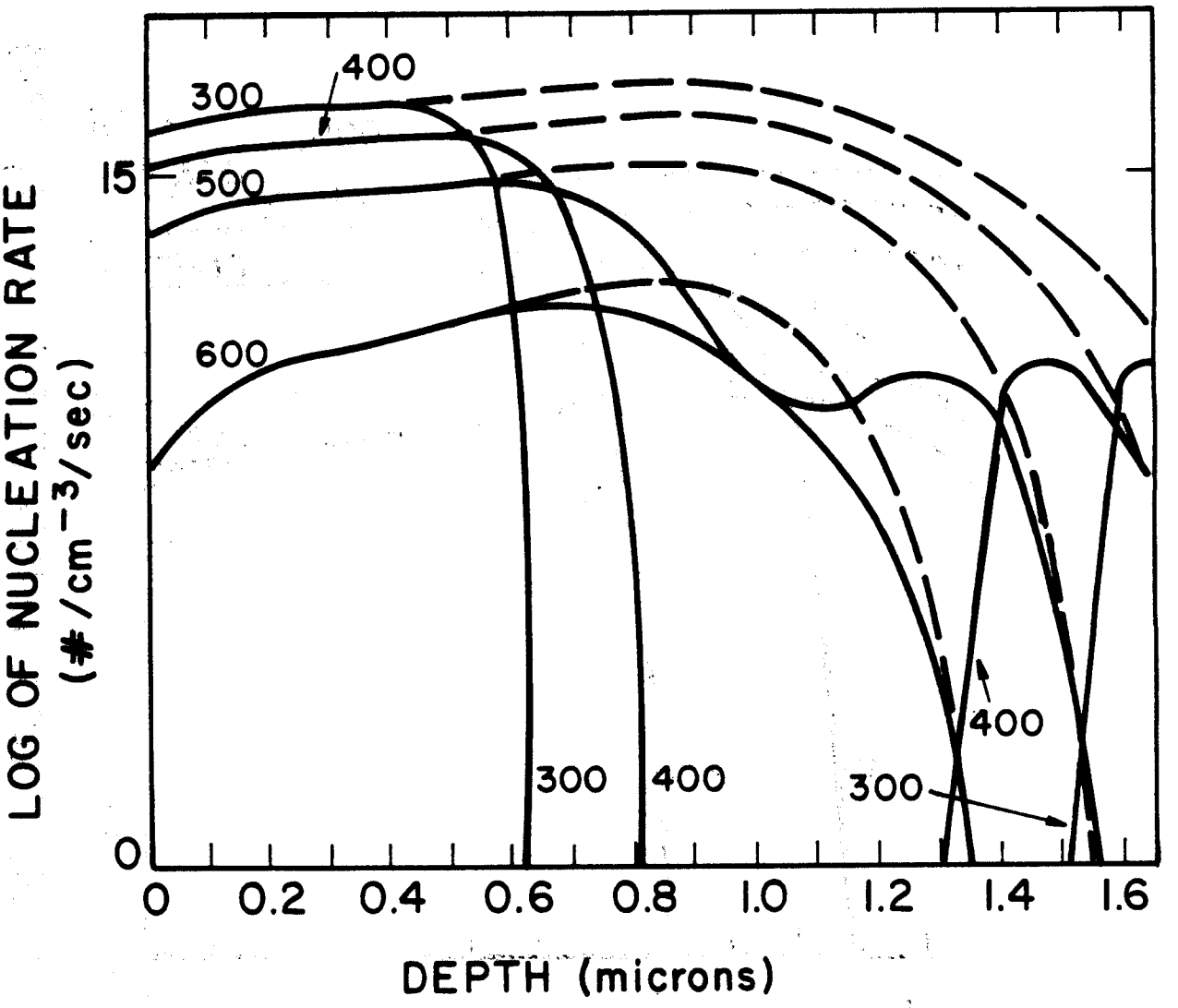

Fig. 11. Void nucleation profile from BRICE data.

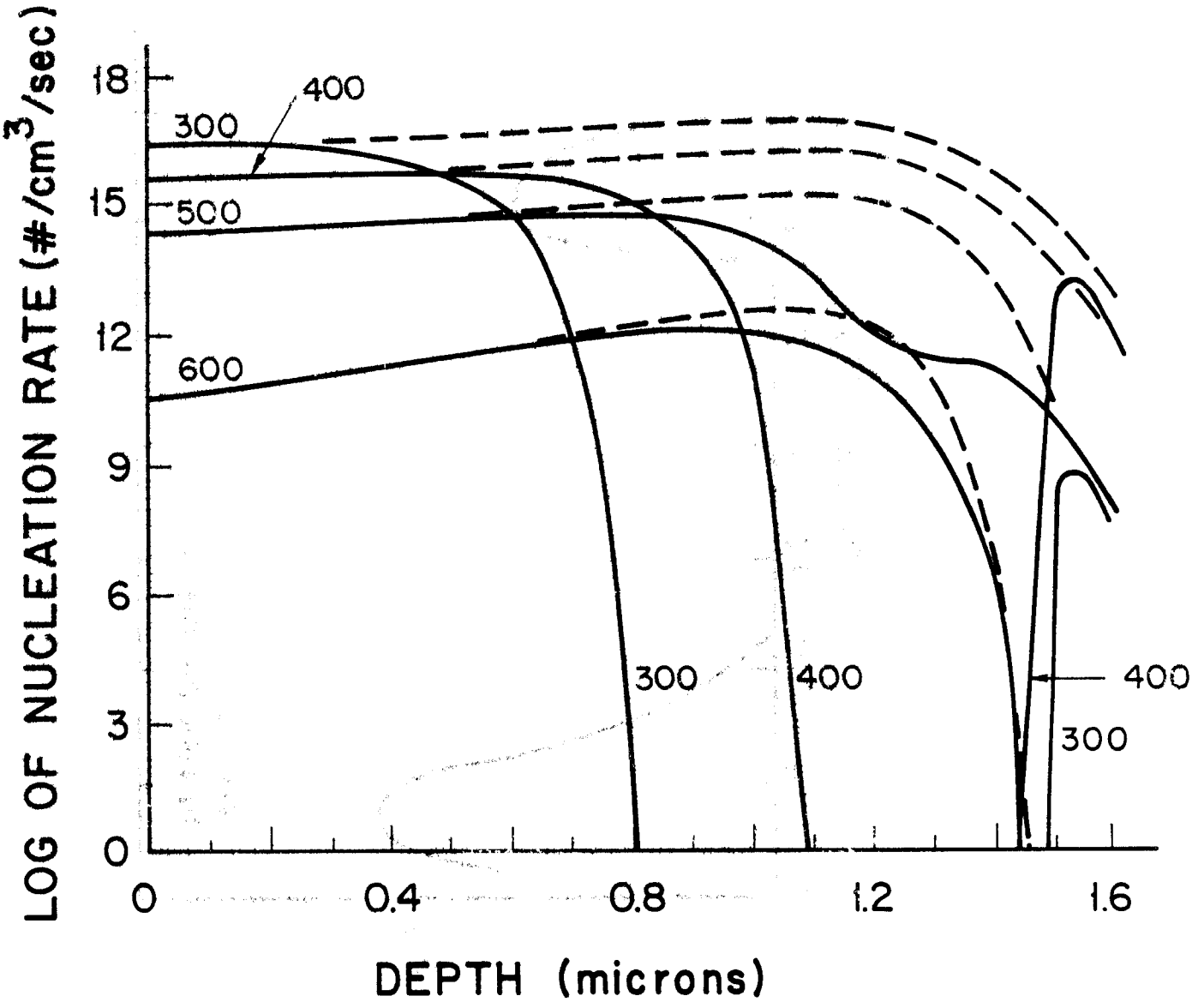

Fig. 12. Void nucleation profile from HERAD data.

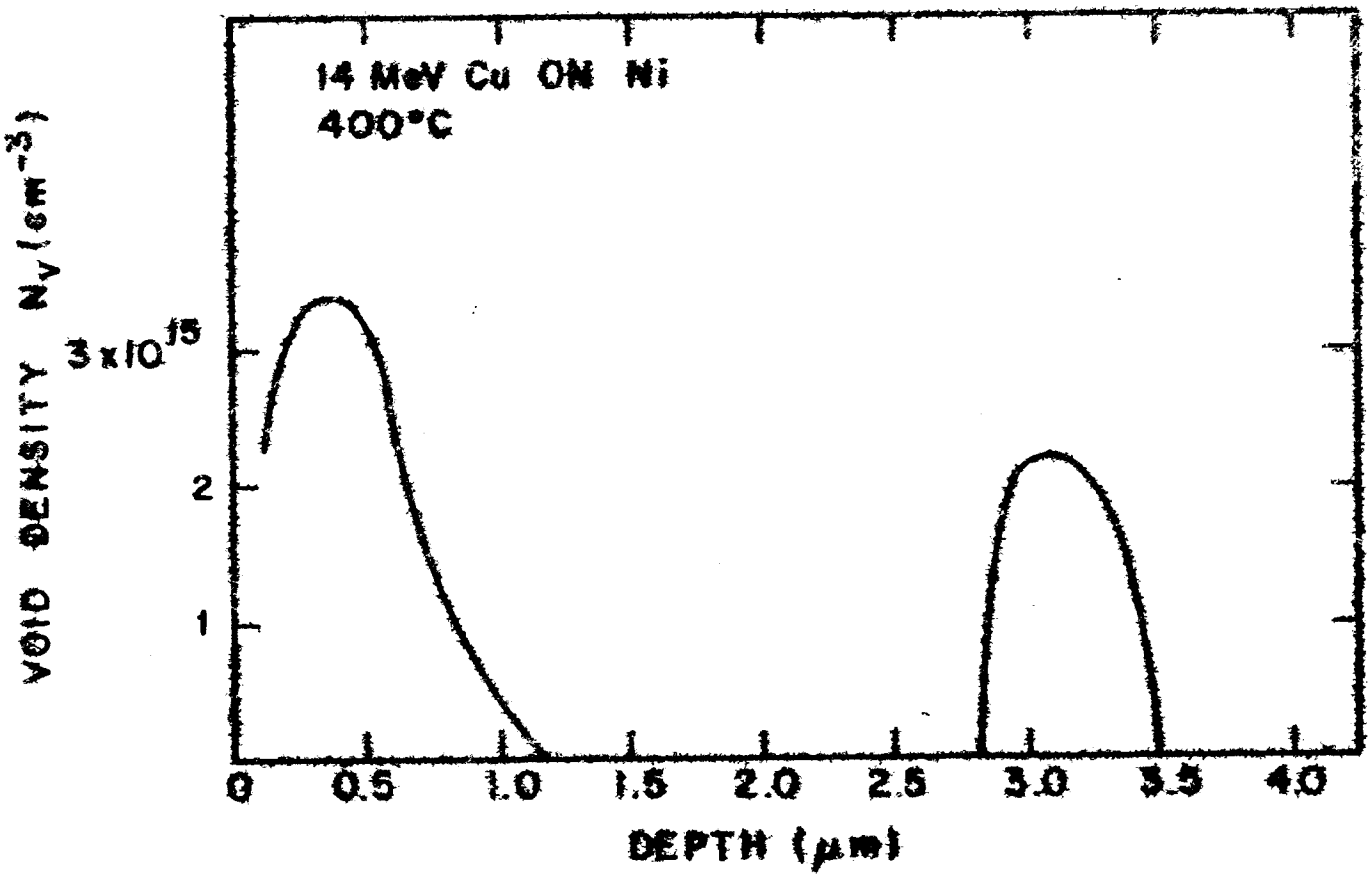

Fig. 13. Void density vs. depth for nickel irradiated at 400°C with 14 MeV Cu-ions to a fluence of about 5 x 10^{16} ions/cm^2.